Proceedings of 10th International Conference on Precision, Meso, Micro and Nano Engineering (COPEN 10)
December 07 – 09, 2017, Indian Institute of Technology Madras, Chennai – 600 036 INDIA

Analytical Simulation and Statistical Modeling of Microdrilling of a Nickel-Based Superalloy

Sabana Azim , S. Gangopadhyay and S. S. Mahapatra

Department of Mechanical Engineering,
National Institute of Technology Rourkela, Odisha,769008, India

Abstract

Microdrilling of nickel-based superalloy is very challenging process due to the material properties, operating conditions, and high quality requirements. The current study described the machinability of Incoloy 825 in microdrilling operation and also the effect of spindle rpm and feed rate on thrust force and torque under flood cooling condition. In order to achieve some of the objectives of the research work, initial study has been under taken aiming at investigating the influence of spindle speed (10000, 20000 and 30000 rpm) and feed (1, 4, 8 and 12 µm/rev) on thrust force and torque. ANSYS simulation of the same process was carried out in order to determine equivalent stress and deformation using thrust force and torque values obtained from the experiment. Surface roughness of the bottom surface of the micro hole also increased with both cutting speed and feed. From the finite element modeling (FEM), it was concluded that deformation and equivalent stress in the microdrill not only increased with cutting parameters, but maximum values were obtained in and around the chisel edge. Statistical analysis was also carried out to develop predictive models for thrust force, torque and surface roughness in microdrilling of Incoloy 825.

Keywords: Microdrilling, Incoloy 825, Simulation, Statistical Analysis, Surface Roughness.

1. INTRODUCTION

Mechanical microdrilling is a process in which material will be removed in micron level with a drill diameter of less than or equal to 500µm. Generally, microdrill is made up of micro grains of tungsten carbide or steel. Compared to mechanical microdrilling, other hole making processes like laser, plasma, electron and ion beam machining have high set up time, high initial investment cost and low material removal rate (MRR), thus are not so economical for small batch production. Microdrilling has wide application in the fields of automobile, aerospace, computer, electronics equipment, medical instrumentation and other precision product industries. Microdrilling is different from macrodrilling primarily in terms of size, cutting mechanism and ratio of uncut chip thickness to edge radius. In micro machining to get minimum chip thickness, the depth of cut needs to be higher than the critical chip thickness to overcome the predominant effect of elastic deformation. Out of all the problematic issues, the measurement of forces is extremely challenging due to the size of tools and small values of the forces.

Micro machining is closely related to the microstructure of the material thus significantly affecting various performance measures like specific cutting forces, dynamic instability and surface finish, since the work material no longer behaves like a homogeneous material. This is due to the fact that tool dimension in micro machining has same order of magnitude with that of size of various grains which have different properties from grain boundaries even for pure metal. This is called size effect and it becomes more pronounced for metallic alloys [1]. Various investigations were carried out in the field of microdrilling with different workpiece materials. The effect of different parameters like drill diameter [2-6], spindle speed and feed rate [1,7-9] was investigated on the hole qualities and surface roughness of hole on Ni-based super alloys and printed circuit board (PCB) using microdrill made up of cemented carbide. Kim et. al [10] studied in deep microdrilling of AISI 1045 and AISI P20 with an aspect ratio of 15, all drills broke while drilling the first hole regardless of the cutting condition because the cutting fluid was not sufficiently supplied and the chips were not removed. It leads to the serious problem issue in microdrilling operation. By using this, a stable drilling condition was obtained for drilling of steel and Al. Imran et. al [9] investigated microdrilling of Inconel 718 under wet cutting conditions. They suggested that subsurface alterations were driven by thermo-mechanical loading, causing plasticity and grain refinement by excessive shear deformation local to the micro machined surface. Hinds and Treanor [11] analyzed stresses in microdrills with a diameter of 0.1 mm using finite element method (FEM) during machining of printed circuit board (PCB). The experimental values of thrust force and torque were utilized as the inputs to FE analysis for determining stresses and deformation at the various sections of the microdrill. Similar approach was presented by Sahoo et.al [12]. Hinds and Treanor [11] presented principal stress isograms on drill cross-sections for different drill geometries and correlated with actual drill life. Shi et. al [13] proposed to obtain temperature distribution in microdrilling process and the temperature drop in retracting process with simulation software. It was found that high temperature concentrated in the regions of cutting edge and chisel edge and it increased with spindle speed and feed. Sahoo et. al [12] indicated that stresses played an important role in influencing hole quality. Hole diameter reduced with increase in feed rate, whereas delamination factor and mean burr thickness increased during microdrilling of PCB. They utilized FE analysis based simulation of deformation and equivalent stresses to explain various characteristics of micro hole. Although some work on microdrilling has been reported on PCB, the same on Ni-based super alloys is relatively fewer. Therefore, the current work is aimed at investigating the influences of spindle speed on cutting forces and torque which are further utilized for determining predictive regression models and simulation of deformation and stresses along the various section of the microdrill. The roughness of bottom surface was also experimentally determined and successfully correlated with the results obtained from FE analysis.

2. EXPERIMENTAL DETAILS

Micro drilling operation was performed using an ultra-high speed micro machining centre in machine tool lab at IIT Bombay (Make: Indian Institute of Technology Bombay,

ISBN: 978-93-80689-28-9

Mumbai, India). A high speed spindle with a speed range of up to 170000 rpm is mounted on a vertical axis (Z axis) with maximum feed rate of 0.06 to 6000 mm/min. Machining operation was carried out under flood environment. Three different levels of spindle speed such as 10000, 20000 and 30000 rpm, four levels of feed i.e. 1, 4, 8 and 12 µm/rev and drilling depth of 1.25 mm were considered for the study. A drill diameter of 0.4 mm was chosen for the experiment. During the operation a tool dynamometer (Make: Kistler; Model: 9256C1) was used to record the forces in X, Y and Z directions. Fig.1. shows a schematic representation of a microdrilling set up. After micro machining the state of the hole was monitored using a 3D surface profilometer (Make: Zeta Instruments, USA). A 3D model of the microdrill was drawn using SOLIDWORKS and imported to ANSYS in IGS format. FE analysis based simulation for deformation and equivalent stress was carried out using ANSYS 15.0 workbench software. Experimental values of thrust force and torque value are used as input data for simulation of deformation and stress. The 3D model microdrill was modelled with an assumption that it is rigid. Both rotational and translational motions were given to the drill along the Z direction. Drilling was simulated as in static structural module. In the static structural module, load and moment were applied on the drill bit [14, 15]. The micro drill after meshing is depicted in Figure 2. The model was then solved for the required output.

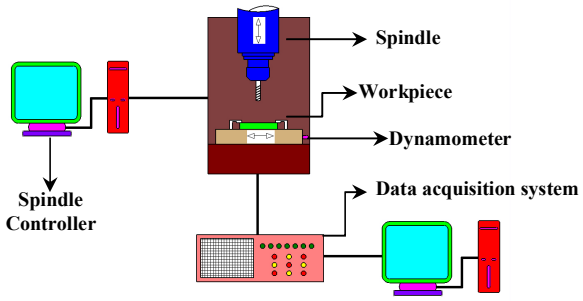

Fig. 1.Micro drilling set up arrangement

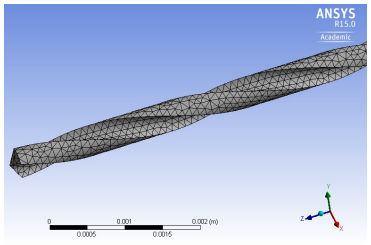

Fig. 2.Meshing of micro drillbit

3. RESULTS AND DISCUSSION

3.1 Cutting Forces

Previous studies on microdrilling exhibited decrease in thrust force (F_z) consistently with rise in cutting speed which was attributed to material softening at high cutting speed. From Fig. 3, significant increase in the thrust force with feed was observed due to an increase in chip load. Elevation in spindle speed causes an increase in thrust force under lowest feed of 1 µm/rev whereas rise in cutting speed under the condition of high feed causes no significant variation in thrust force. It is interesting to note that two mutually conflicting situations arise with elevation in cutting speed. In addition to thermal softening, deformation induced strain hardening is a typical phenomenon in case of machining in Ni-based super alloy. Therefore these two mechanisms tends to balance each other at feed rates of 4, 8 and 12 µm/rev. Hence, strain hardening due to larger contribution of edge rounding and deformation might have led to increasing trend with spindle speed. Similar trend has been obtained with torque under lowest feed of 1 µm/rev as indicated in Fig.4. Owing to significant fluctuation of torque, maximum peak to valley was considered and demonstrated in Fig.4 such technique has been recommended by Rahamathullah and Shunmugam [2].

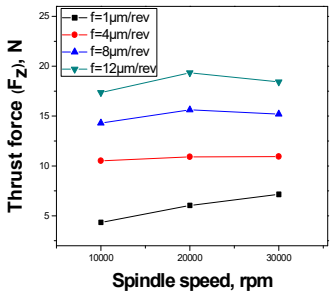

Fig. 3.Variation of thrust force (F_z) with spindle speed and feed rate

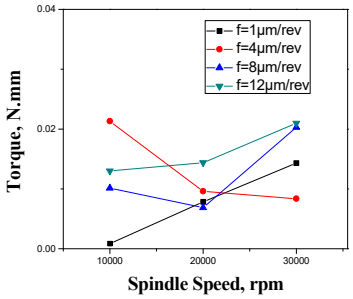

Fig. 4.Variation of torque with spindle speed and feed rate

It is known that radial forces F_x and F_y do not have much significance on the performance of drilling under macro regime. However, their effect is amplified during microdrilling and they occur due to error in rotational symmetry of the drill lips and margin. These forces are particularly undesirable since they cause wandering of the drill tip at the entrance making it prone to breakage. These two forces F_x and F_y are plotted in Fig.5 and Fig.6. General trend shows rising trend with cutting speed. Higher value of forces at 1µm/rev compared to 4µm/rev is again explained by dominance of ploughing effect due to lower undeformed chip thickness than edge radius.

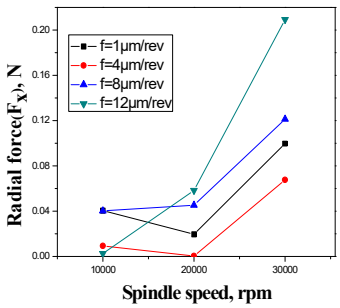

Fig. 5.Variation of radial force with speed rpm and feed rate

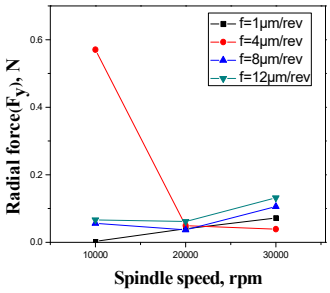

Fig. 6.Variation of radial force with speed rpm and feed rate

3.2 Predictive regression models

By using the experimental values which are calculated by arithmetic mean are utilized for development of surface plots. Input parameters are spindle speed (A) and feed (B), and output responses are thrust force (F_z), radial forces (i.e. F_x, F_y) and torque. Comparative analysis of different models was carried out but in quadratic model found the significant with coefficient of determination (R^2). The quadratic regression equations are shown below (Eq.1 to Eq.4)

$$\textit{Thrust force } (F_z) = 2.89926+6.51481E\text{-}005GA+1.79031GB-0.051214GB^2 \quad (1)$$

$$\textit{Radial force } (F_x) = 0.16325-1.31780E\text{-}005GA-0.023759GB+9.41329E\text{-}007GAGB+3.47665E\text{-}01GA^2+1.24787E\text{-}003GB^2 \quad (2)$$

$$\textit{Radial force } (F_y) = 0.52636-4.36186E\text{-}005GA+0.014099GB+9.41329E\text{-}007GAGB+8.34826E\text{-}010GA^2-2.60779E\text{-}003GB^2 \quad (3)$$

$$Torque=0.14091-1.20670E\text{-}005GA-0.023847GB+7.62833E\text{-}007GAGB+2.55400E\text{-}010GA^2+1.11789E\text{-}003GB^2 \quad (4)$$

Effect of spindle speed and feed with different output responses are shown in Fig.7 to Fig.10 after calculating the predicted values. When these predicted values were compared with experimental values, they showed close similarities (94.1% R^2).

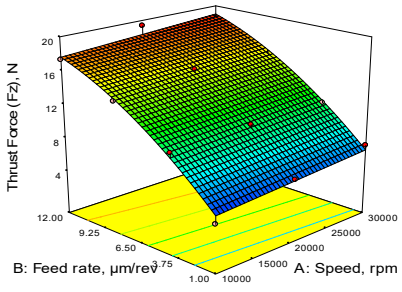

Fig. 7.Effect of speed rpm and feed rate on thrust force (F_z)

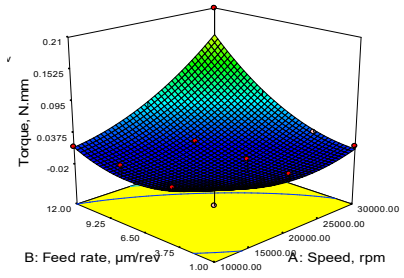

Fig. 8.Effect of speed rpm and feed rate on torque

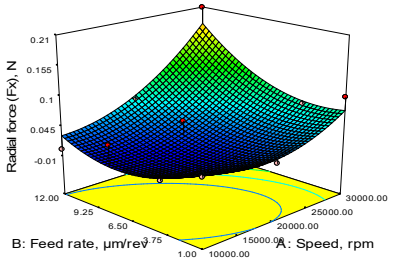

Fig.9.Effect of speed rpm and feed rate on radial force (F_x)

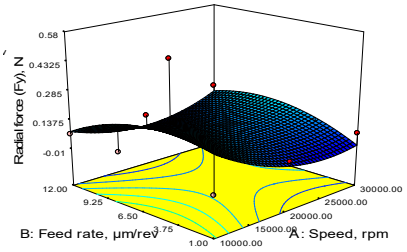

Fig. 10.Effect of speed rpm and feed rate on radial force (F_y)

3.3 Simulation analysis

As described earlier thrust force (F_z) and torque values obtained through experimentation were utilised in the finite element model for simulation. Deformation and equivalent stress profile were determined. Fig. 13 shows the deformation profile of the microdrill during machining of Incoloy 825. Evidently, primary cutting edge and chisel edge were subjected to maximum deformation in Fig.14. This might be explained by the fact that prior pilot hole was not drilled leading to greater thrust encountered by chisel edge and cutting edge. Slight drifting motion due to very small value of F_x and F_y might also have caused small degree of deformation at the entrance [5]. According to Hinds et. al [11], brittle fracture is the dominant mode of failure for cemented carbide microdrill. Therefore, equivalent stress was simulated and presented in Fig.15. It is again evident that chisel edge experienced maximum equivalent stress under different cutting condition. A portion of the chisel edge called secondary cutting edge is responsible for material removal and the remaining part tries to indent or push the material ahead. Simulated values of equivalent stress and deformation are plotted with different spindle speed and feed in Fig.11 and Fig.12.

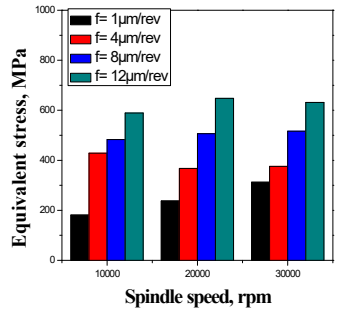

Fig. 11.Variation of equivalent stress with speed rpm and feed rate

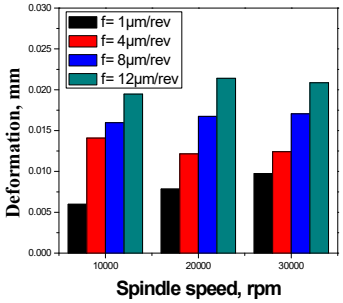

Fig. 12.Variation of deformation with speed rpm and feed rate

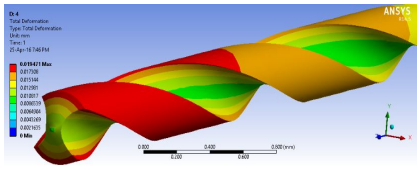

Fig. 13.Representative image of deformation at condition (10000 rpm and 12µm/rev)

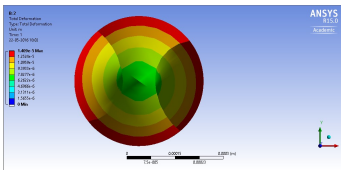

Fig. 14.Total deformation in axial and diametric plane at condition (10000 rpm, 12µm/rev)

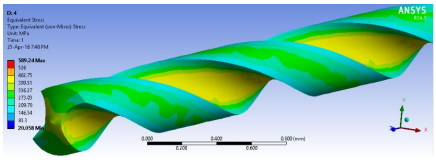

The figure clearly shows increasing trend of surface roughness with both feed and cutting speed. While higher feed always produced rougher surface, rising trend of R_a with spindle speed might be attributed to high strain hardening tendency and consequent rise in deformation at the chisel edge as shown in Fig.14.

Fig. 15.Representative image of equivalent stress at condition (10000 rpm, 12µm/rev)

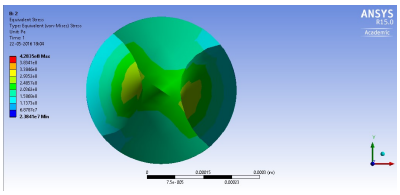

Fig. 16.Maximum principal stress in axial and diametric plane at condition(10000 rpm, 12µm/rev)

3.3 Surface roughness

Owing to difficulty associated with the measurement of surface roughness of hole surface; attempt was made to determine the same at the bottom of the hole using a non-contact type 3D surface profilometer. The surface roughness would primarily reveal the contribution of chisel edge since pilot hole was not drilled apriori. Since finite element simulation has demonstrated that the deformation and stress at and around chisel edge increased with cutting speed and feed, it is reasonable that they would have considerable effect on surface roughness measured at the bottom surface. Fig.17 depicts a representative image of the surface profile and the values of average surface roughness (R_a) were plotted in Fig.18.

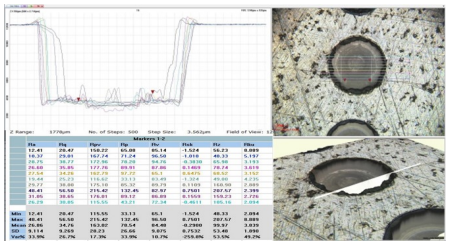

Fig. 17.Representative image of surface profile of microdrill

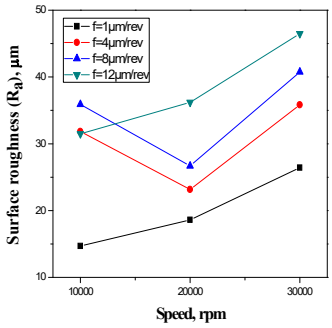

Fig. 18.Variation of surface roughness with speed rpm and feed rate

4 CONCLUSIONS

The present research work investigated the influence of cutting parameters on various micro machining characteristics during microdrilling of Incoloy 825. The following conclusions are derived from the study.

- Apart from expected increase in thrust force, radial forces and torque with feed, they showed rising trend with cutting speed as well. This was attributed to the prominent strain hardening effect of Incoloy 825 which increases with cutting speed.
- Surface roughness of the bottom surface of the micro hole also increased with both cutting speed and feed.
- From the FE modeling it was concluded that deformation and equivalent stress in the microdrill not only increased with cutting parameters, but maximum values were obtained in and around the chisel edge.

ACKNOWLEDGMENT

The authors are grateful to Prof. Ramesh Singh of IIT Bombay and his research group for kindly providing the micro machining facility and cooperation rendered during experiment.

References

[1] M. Imran, P. T. Mativenga, S. Kannan, and D. Novovic, "An experimental investigation of deep-hole micro drilling capability for a nickel-based superalloy", DOI: 10.1243/09544054JEM1217.

[2] I. Rahamathullah and M. S. Shunmugam," Thrust and torque analyses for different strategies adapted in microdrilling of glass-fibre-reinforced plastic", DOI: 10.1243/09544054JEM2151.

[3] L. Zheng, C. Wang, L. Yang , Y. Song and L. Fu," Characteristics of chip formation in the micro-drilling of multi-material sheets", *International Journal of Machine Tools & Manufacture,* 52: 40–49, (2012).

[4] I. Rahamathullah and M. S. Shunmugam," Analyses of forces and hole quality in micro-drilling of carbon fabric laminate composites", *Journal of Composite Materials,* 47: 1129–1140, (2012).

[5] K. Patra, R. S. Anand, M. Steiner and D. Biermann," Experimental Analysis of Cutting Forces in Microdrilling of Austenitic Stainless Steel (X5CrNi18-10)", *Materials and Manufacturing Processes*, 30: 248–255, (2015).

[6] H. Watanabe, H. Tsuzaka and M. Masuda, "Microdrilling for printed circuit boards (PCBs)—Influence of radial run-out of microdrills on hole quality", *Precision Engineering,* 32: 329–335, (2008).

[7] J. S. Nam, P. H. Lee and S. W. Lee," Experimental characterization of micro-drilling process using nano fluid minimum quantity lubrication", *International Journal of Machine Tools & Manufacture*, 51: 649–652, (2011).

[8] M. Imran , P. T. Mativenga , A. Gholinia and P. J. Withers," Comparison of tool wear mechanisms and surface integrity for dry and wet micro-drilling of nickel-base superalloys", *International Journal of Machine Tools & Manufacture*, 76: 49–60, (2014).

[9] M. Imran, P. T. Mativenga, A. Gholinia and P. J. Withers," Evaluation of surface integrity in micro drilling process for nickel-based superalloy", *International Journal of Machine Tools & Manufacture*, 55: 465–476, (2011).

[10] D. W. Kim, Y. S. Lee, M. S. Park and C. N. Chu ," Tool life improvement by peck drilling and thrust force monitoring during deep-micro-hole drilling of steel", *International Journal of Machine Tools & Manufacture,* 49: 246–255, (2009).

[11] B.K. Hinds and G.M. Treanor," Analysis of stresses in micro-drills using the finite element method", *International Journal of Machine Tools & Manufacture,* 40: 1443–1456, (2000).

[12] S. Sahoo, A. Thakur and S. Gangopadhyay," Application of Analytical Simulation on Various Characteristics of Hole Quality during Micro-Drilling of Printed Circuit Board", *Materials and Manufacturing Processes*, 31: 1927–1934, (2016).

[13] H. Shi, H. Li and S. Chen," Temperature simulation and its application in on-line temperature measurement of a micro drill bit", [DOI 10.1108/CW-10-2014-0045].

[14] M. M. Shokrieh and D. Rezaei, Analysis and optimization of a composite leaf spring, *Composite Structures,* 60: 317–325, (2003).

[15] P. V. S. Teja, S. Prakash, B. N. Prasad and G. Elijah, Finite element analysis in drilling GFRP composites, *Indian Journal of Science and Technology,* 8(15): 1–5, (2015)